Science and Technology for Energy Transition **79**, 63 (2024)

https://doi.org/10.2516/stet/2024065

**Decarbonizing Energy Systems: Smart Grid and Renewable Technologies**
Fang Rui-ming and Qiangqiang Liao (Guest Editors)

Available online at:
stet-review.org

REGULAR ARTICLE OPEN ACCESS

# Modelling cost-effective of electric vehicles and demand response in smart electrical microgrids

Shaikh Hasibul Majid[1], Alhussein G. Alkhayer[2], Shavan Askar[3], Asha Rajiv[4], Sandeep Singh[5,6], Sarabpreet Kaur[7], Ashish Singh[8], Layth Hussein[9,10,11], Yersi S. Romaina[12,*], and Raul Perz[12]

[1] Department of Electrical Engineering, University of Tabuk, Tabuk, Saudi Arabia
[2] Department of Electrical Engineering Techniques, Al-Amarah University College, Maysan, Iraq
[3] Erbil Polytechnic University, Erbil Technical Engineering College, Information System Engineering Department, Erbil, Iraq
[4] Department of Physics & Electronics, School of Sciences, JAIN (Deemed to be University), Bangalore, Karnataka, India
[5] School of Engineering, Bahra University, Waknaghat, Solan, Himachal Pradesh, India
[6] Faculty of Engineering, Sohar University, PO Box 44, Sohar, PCI 311, Oman
[7] Department of Electronics and Communication Engineering, Chandigarh College of Engineering, Chandigarh Group of Colleges, Jhanjeri, Mohali, 140307, Punjab, India
[8] NIMS School of Electrical and Electronics Engineering, NIMS University Rajasthan, Jaipur, India
[9] Department of Computers Techniques engineering, College of Technical Engineering, The Islamic University, Najaf, Iraq
[10] Department of Computers Techniques Engineering, College of Technical Engineering, The Islamic University of Al Diwaniyah, Al Diwaniyah, Iraq
[11] Department of Computers Techniques Engineering, College of Technical Engineering, The Islamic University of Babylon, Babylon, Iraq
[12] Department of Energy, Madrid Institute for Advanced Studies in Energy, Madrid, Spain

Received: 28 April 2024 / Accepted: 7 August 2024

**Abstract.** The intermittent nature of renewable energy sources such as solar and wind power can lead to fluctuations in the supply of electricity within a microgrid, making it difficult to maintain a consistent and reliable power supply. This can result in disruptions to critical operations and services that rely on a stable source of energy. Additionally, the integration of electric vehicles into a microgrid introduces another layer of complexity, as the charging and discharging of these vehicles can create additional demand and strain on the grid. This can lead to imbalances in the supply and demand of electricity, further impacting the stability and efficiency of the microgrid. This paper presents an approach for the optimal behaviour of electric vehicles and demand side for an electrical microgrid. The proposed approaches are multi-domain attention-dependent conditional generative adversarial network (MDACGAN) and seahorse optimization (SHO) techniques. The primary goal of the suggested method is to reduce the operational cost of the system, maximize the utilization of solar power and reduce electricity fluctuations. The economic dispatch model manages the fluctuation of renewable energy sources through the implementation of suggested techniques to handle unpredictability. The effectiveness of this approach is evaluated using the MATLAB platform and compared against other methods. The suggested technique demonstrates superior outcomes across all methodologies. Based on the findings, it can be inferred that the suggested technique boasts a lower cost in comparison to other methods.

**Keywords:** Electric vehicles, Demand side response, Hybrid approaches, Operational cost, Transferable load.

## 1 Introduction

### 1.1 Aims and motivations

The increasing global need for electricity has brought environmental and social concerns to the forefront [1]. Traditional power plants burning fossil fuels have caused extensive environmental damage, and the outdated power grid faces challenges of high expenses and poor efficiency [2–4]. Consequently, electric vehicles, which support clean energy generation with renewable electricity, have gained widespread acceptance worldwide [5, 6]. A microgrid is a network that produces and delivers electricity through different sources [7, 8]. It plays a crucial role in power systems because of its strong security measures, high use of renewable energy, and cost-effectiveness [9–11]. Nevertheless,

* Corresponding author: yersi.luis.ro@gmail.com

the unpredictable nature of green energies poses challenges to maintaining balance in the microgrid, as well as in efficiently managing the system [12, 13]. Furthermore, the integration of renewable energy sources such as solar, wind, and hydropower into the grid is essential in reducing use of fossil fuels [14, 15]. These sources of energy are abundant, clean, and sustainable, making them a viable alternative to traditional forms of electricity generation [16–18]. By investing in renewable energy infrastructure and improving energy storage capabilities, countries can ensure more reliable and resilient energy systems for the future [19, 20]. In addition to technological advancements, changes in consumer behaviour and energy efficiency measures are also key in reducing electricity demand and promoting sustainability [20]. Energy conservation practices, such as using energy-efficient appliances, implementing smart home technology, and adopting energy-saving habits, can help lower overall electricity consumption and reduce the need for additional fossil fuel-based power generation [21, 22]. Overall, the transition to a cleaner and more sustainable energy system requires a multi-faceted approach that includes advancements in technology, policy changes, and individual actions [22, 23]. By working together to reduce our reliance on fossil fuels and embrace renewable energy sources, energy organizations can create a more sustainable future for generations to come. Therefore, integrating electric vehicles in the microgrid operation can serve as a vital decentralized optimal power supply [23–25].

### 1.2 Related studies

Past studies on microgrid dispatching have primarily concentrated on various objective functions aimed at optimizing the results of dispatching. Multi-objective functions such as the environmental cost and the generation cost of the microgrid are commonly explored. Factors like the total life cycle expenses, wind desertion rate of a grid-connected microgrid, operating costs, and reliability are also taken into consideration [26]. The support from the distribution network has significantly boosted the operational dependability of the microgrid [27]. Nevertheless, the distribution network of a microgrid is mainly fuelled by fossil fuels, leading to severe environmental pollution. As a result, microgrids consist of both fuel-powered and renewable energy devices [28]. By integrating renewable energy sources, the microgrid's environmental efficiency is improved by reducing fuel consumption [29]. While these sustainable energy devices are expensive, they serve the primary objectives of the microgrid, which are economic and environmental protection [30]. The system's environmental protection is boosted by the optimal unit output, leading to increased utilization of renewable energy sources [31]. Economic incentives can be used to regulate the random variables of loads in microgrids, significantly impacting their stability [32]. To fully exploit the advantages of load on MGs, it is essential to create demand response mechanisms [33]. The primary obstacle for these resources is the unpredictability of their power output due to the random nature of natural parameters [34]. Ignoring the ambiguity surrounding microgrid energy management can lead to inaccurate predictions of resource output values. As a result, researchers have proposed various techniques, including deterministic and non-deterministic methods [35]. Managing power systems is becoming more challenging due to the integration of electric vehicles into the grid. Improving grid management efficiency is essential, especially with the abundance of renewable energy sources [36]. Previous methods tend to focus on local areas and lack a robust global search engine, which are two major limitations [37]. The inconsistent availability of renewable energy and the uncertainty surrounding its usage is having a detrimental effect on the reliable operation of a microgrid. Additionally, integrating electric vehicles as variable power consumers can greatly disrupt the effective functioning of the microgrid. Currently, economic and environmental considerations are the primary focus of microgrid optimization dispatches [38].

### 1.3 Contributions of this paper

The study aims to improve the microgrid's advantages by focusing on the microgrid's operational expenses and environmental sustainability. Therefore, our contributions in this paper can be summarized as follows:

1. This paper presents a novel hybrid approach for managing the charging and discharging patterns of electric vehicles, as well as implementing load management in a microgrid system.
2. The approach combines such as multi-domain attention-dependent conditional generative adversarial network (MDACGAN) and seahorse optimization algorithm (SHO) techniques are proposed.
3. The method proposed is designed to reduce the microgrid's expenses, optimize the use of solar power, and decrease energy fluctuations between the microgrid and the main grid.

## 2 Overview of proposed microgrid

Figure 1 displays a grid-connected micro-grid to evaluate the suggested strategy. Photovoltaic (PV) panels generate electricity from sunlight, which is then stored in the energy storage system for later use. The electric vehicle is also connected to the micro-grid, allowing it to be charged using the renewable energy generated by the PV panels. The load represents the energy demand from various devices within the microgrid. The communication link enables the energy management system to gather real-time data on the energy production from the PV panels, the energy consumption of the electric vehicle, and the overall energy demand from the load. This data is then analyzed to determine the most efficient energy set points for the main grid, resources, and demand within the microgrid. By optimizing the energy set points, the micro-grid can minimize its reliance on the main grid, maximize the use of renewable energy sources, and ensure that the energy demand from the load and electric vehicle is met without any interruptions. This strategy

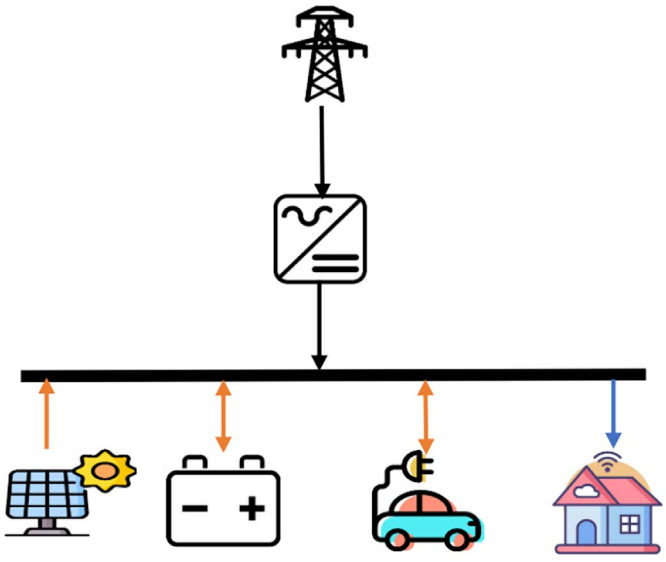

**Fig. 1.** Overview of proposed microgrid.

allows for the efficient and sustainable operation of the microgrid, reducing its environmental impact and overall energy costs.

## 2.1. Modelling PV

The mathematical model for the PV considering the influence of both temperature and sun irradiation on solar output power are extracted from References [39].

## 2.2. Modelling electric vehicle

Modelling electric vehicles based on probability density function is as follow [40]:

$$E_1(t) = \begin{cases} \frac{4}{\sqrt{2\pi}\sigma_1} e^{-\frac{(s+96-\mu_1)^2}{2\sigma_1^2}} & 0 \le s \le \mu_1 - 48 \\ \frac{4}{\sqrt{2\pi}\sigma_1} e^{-\frac{(s-\mu_1)^2}{2\sigma_1^2}} & 0 \le s \le \mu_1 - 48 \end{cases}. \quad (1)$$

Where:
$\mu_1$ = Charging of electric vehicles.
$\sigma$ = Standard deviation.
In following, the probability density function is as follows:

$$E_g(\varsigma) = \frac{1}{\varsigma} \frac{1}{\delta_g \sqrt{2\pi}} \exp\left(-\frac{\left(\ln \varsigma - \mu_g\right)^2}{2\delta_g^2}\right). \quad (2)$$

Where:
$\mu_g$ = Daily mileage of electric vehicles.
$\sigma_1$ = Standard deviation of daily mileage.
It is essential to consider the resistive forces when modelling electric vehicles to ensure they can effectively overcome them. The force that propels a vehicle forward is referred to as tractive effort and is transmitted to the ground through the wheels.

The force of rolling resistance grows as the vehicle weight increases, mainly due to the friction between the tyres and the road. These forces are as follows:

$$E_{\mathrm{RR}} = \mu_{\mathrm{RR}} \times M. \quad (3)$$

Where:
$E_{\mathrm{RR}}$ = Rolling resistance force.
$\mu_{\mathrm{RR}}$ = Coefficient of resistance.
M= Electric vehicles with mass.
And force of hill climbing is:

$$E_{\mathrm{LA}} = M \times A. \quad (4)$$

Where:
A = Area of motor.
The torque of the motor is:

$$T_{\mathrm{TE}} = E_{\mathrm{LA}} \times \frac{R}{g}. \quad (5)$$

Where:
$R$ = Radius of the wheels.
$g$ = Gears ratio.

## 2.3. Modelling demand response

Transferable Load (TL) is the capacity to move demand from one time to another time. Modelling demand response based on TL approach is as follows [41]:

$$G_{\mathrm{in}}(t) = \sum_{K=1}^{M_{\mathrm{TL}}} \chi_K(t) G_{1\cdot K} + \sum_{b=1}^{b_{\max}-1} \times \sum_{K=1}^{M_{\mathrm{TLe}}} \chi_K(t-b) G(b+1) \cdot K. \quad (6)$$

$$G_{\mathrm{out}}(t) = \sum_{K=1}^{M_{\mathrm{TL}}} Z_K(t) G_{1\cdot K} + \sum_{b=1}^{b_{\max}-1} \times \sum_{K=1}^{M_{\mathrm{TLe}}} Z_K(t-b) G(b+1) \cdot K. \quad (7)$$

Where:
$G_{\mathrm{in}}(t)$ = Transfer-in value.
$G_{\mathrm{out}}(t)$ = Transfer-out value.
$M_{\mathrm{TL}}$ = TL numbers
$M_{\mathrm{TLe}}$ =TL numbers with longer time operation.
$b_{\max}$ = Maximum operation time
$\chi_{\mathrm{K}}(t)$ = Quantity of load transfer-in.
$Z_{\mathrm{K}}(t)$ = Quantity of load transfer-out.
$G_{1\cdot K}$ = Energy consumption of TL.
The representation of the transfer subsidy cost paid by the microgrid system for TL participation is as follows:

$$C_{\mathrm{TL,COST}} = \sum_{s=1}^{S} G_{\mathrm{in}}(t) \times C_{\mathrm{TL}}. \quad (8)$$

Where:
$C_{\mathrm{TL,COST}}$ = Cost of TL.
$C_{\mathrm{TL}}$ = Unit price of TL.

### 2.4. Modelling energy storage system

Modelling of storage system in this study is done considering battery modelling. The battery storage's state of charge (SOC) plays a vital role in optimizing microgrid operation. The changes in SOC during the battery's charging and discharging processes, along with the intricate derivation of mathematical models for charging and discharging, are key factors to consider [42]:

$$\mathrm{SOC}(t) = (1-\delta)\cdot \mathrm{SOC}(t-1) + p_{\mathrm{BS}}(t)\Delta t \eta_{\mathrm{c}}/F_{\mathrm{se}} \quad (9)$$

$$\mathrm{SOC}(t) = (1-\delta)\cdot \mathrm{SOC}(t-1) + p_{\mathrm{BS}}(t)\Delta t/F_{\mathrm{se}}\eta_{\mathrm{d}}. \quad (10)$$

Where:
$\mathrm{SOC}(t)$ = SOC of battery in time $t$.
$p_{\mathrm{BS}}(l)$= Energy output of battery.
$\delta$ = Self-discharge power of battery.
$\eta_{\mathrm{c}}$ and $\eta_{\mathrm{d}}$ = efficiencies of battery in the charging and discharging modes.
$F_{\mathrm{se}}$ = Battery capacity.
Also, there are costs of battery as follows:

$$C_{\mathrm{BS,OM}} = |P_{\mathrm{BS}}(t)| \times K_{\mathrm{OM,BS}} \quad (11)$$

$$C_{\mathrm{BS,LOSS}} = M_{\mathrm{D}} \times (C_{\mathrm{COST,CHANGE}}/M_{\mathrm{Dm}}). \quad (12)$$

Where:
$C_{\mathrm{BS,OM}}$ = Operating and maintenance cost.
$C_{\mathrm{BS,LOSS}}$ = Costs of charging and discharging loss.
$K_{\mathrm{OM,BS}}$ = Operation cost coefficient
$C_{\mathrm{COST,CHANGE}}$ = Cost of battery loss in charge-to-discharge modes.
$M_{\mathrm{D}}$ and $M_{\mathrm{DM}}$ = Number of cycle and number of nominal cycles of battery.

## 3 Modelling objective function

The objective function is modelled as follows:

$$E = \min\left[C_{\mathrm{ES,COST}} + C_{\mathrm{EV,COST}}, C_{\mathrm{Grid,COST}} + C_{\mathrm{TL,COST}}\right] \quad (13)$$

$$C_{\mathrm{ES,COST}} = C_{\mathrm{ES,OM}} + C_{\mathrm{ES,LOSS}} \quad (14)$$

$$C_{\mathrm{EV,COST}} = \left|\sum_{s}^{S}(\mathrm{EV}_{\mathrm{load}}(s) + P_{\mathrm{EV}}(s)) \times C_{\mathrm{EV}}\right| \quad (15)$$

$$C_{\mathrm{Grid,COST}} = C_{\mathrm{Grid,price}} + C_{\mathrm{grid,EN}}. \quad (16)$$

Where:
$C_{\mathrm{EV,COST}}$ = Electric vehicles cost.
$C_{\mathrm{ES,COST}}$ = Battery cost.
$C_{\mathrm{Grid,COST}}$ = Main grid cost.
$C_{\mathrm{Grid,price}}$ = Cost of main grid connect-line power.
$C_{\mathrm{grid,EN}}$ = Pollution cost.

### 3.1 Modelling constraints

Modelling constraints of microgrid are given as follows:

#### *3.1.1 Constraints of energy storage system*

The constraints of the energy storage system are as follows:

$$\mathrm{SOC}_{\mathrm{MAX}} \le \mathrm{SOC}(s) \le \mathrm{SOC}_{\mathrm{MIN}} \quad (17)$$

$$p_{\mathrm{ES}}^{\mathrm{MIN}} \le p_{\mathrm{ES}}(s) \le p_{\mathrm{ES}}^{\mathrm{MAX}}. \quad (18)$$

Where:
$p_{\mathrm{ES}}^{\mathrm{MAX}}$and $p_{\mathrm{ES}}^{\mathrm{MIN}}$= Maximum and minimum power output.

#### *3.1.2 Constraints of demand response*

The constraints of demand response are as follows:

$$\begin{cases} x_{TL}(s) \le \chi_{TL}(s) \\ \sum_{s=1}^{S} p_{\mathrm{in}}(s) = \sum_{s=1}^{S} p_{\mathrm{out}}(s) \end{cases}. \quad (19)$$

Where:
$x_{\mathrm{TL}}(s)$= Amount of TL.
$\chi_{\mathrm{TL}}(s)$ = TL capacity.

#### *3.1.3 Constraints of power exchange*

The constraints of power exchange between the microgrid and the main grid are as follows:

$$p_{\mathrm{Grid}}^{\mathrm{MIN}} \le p_{\mathrm{Grid}}(s) \le p_{\mathrm{Grid}}^{\mathrm{MAX}}. \quad (20)$$

Where:
$p_{\mathrm{Grid}}^{\mathrm{MAX}}$ and $p_{\mathrm{Grid}}^{\mathrm{MIN}}$ = maximum and minimum power exchange.

## 4 Optimization method

The approach suggested for enhancing energy efficiency in the microgrid integrates the SHO and MDACGAN methods. By leveraging the SHO and MDACGAN techniques, the optimal dispatch model is improved while considering the microgrid's operation. This integration leads to decreased operational costs and enhanced energy utilization. Results from simulations confirm the efficacy of the proposed approach, demonstrating a notable reduction in errors when compared to conventional control methods. The SHO-MDACGAN algorithm introduced in this research delivers superior results compared to prior studies.

### 4.1 SHO optimization method

This segment delves into the utilization of SHO for optimization. Drawing from the hunting, swimming, and reproduction habits of seahorses in the ocean, the SHO technique was created. It integrates the concepts of exploration and exploitation, reflecting the social interactions of seahorses

as they search for food and navigate their environment. The algorithm's structure is inspired by the stages of seahorse reproduction, with the final phase commencing after the initial two components are completed. A comprehensive explanation of the SHO approach is outlined below [43]:

*First Step:* Initializing
Set up the input data.

*Second Step:* Random Generation
Following initialization, the fitness function was subjected to randomization using the SHO method, as outlined in equation (21).

$$z_s = \begin{bmatrix} Z_{1,j} & Z_{1,Dim-1} & \cdots & Z_{1,H} \\ Z_{2,j} & Z_{2,Dim-1} & \cdots & Z_{2,H} \\ \cdots & \cdots & \cdots & \cdots \\ Z_{n,j} & Z_{n,Dim-1} & \cdots & Z_{n,H} \end{bmatrix}. \quad (21)$$

Where:
$Z_s$ = Population matrix.
$n$ = Population size.
$H$ = Variables.

*Third Step:* Fitness Function
The objective function impacts the level of fitness. The fitness function is defined as:

$$\text{Fitness} = \text{MIN}(E). \quad (22)$$

*Fourth Step:* Behaviour of Movement
Seahorses' movement pattern is used as a model for the standard distribution. Two instances are given to help find a middle ground between exploring and exploiting, with a boundary point at 0. The mathematical expression for exploration ($\sigma$) is as follows:

$$\sigma = \left( \frac{\Gamma(1\overleftrightarrow{} + \lambda) \times sin\left(\frac{\pi\lambda}{2}\right)}{\Gamma\left(\frac{1\overleftrightarrow{}+\lambda}{2}\right) \times \lambda \times 2\left(\frac{\lambda-1}{2}\right)} \right). \quad (23)$$

Where:
$\lambda$ = Random number.
Exploitation in seahorses involves mimicking the Brownian motion of another seahorse to enhance their movement through ocean waves.

$$\beta_j = \frac{1}{\sqrt{2\pi}} \exp\left(-\frac{Z^2}{2}\right). \quad (24)$$

Where:
$\beta_j$ = Coefficient of random walk.

*Fifth Step:* Foraging Behaviour
Seahorses searching for food can either succeed or fail. Success happens when the seahorse moves faster than the prey ($r_2 > 0.1$), while failure occurs when the opposite is true. The standards for measuring success and failure in seahorses' quest for food are as stated here:

$$\alpha = \left(1 - \frac{s}{S}\right)^{\frac{2s}{S}} \quad (25)$$

Where:
$S$ = Number of iterations.

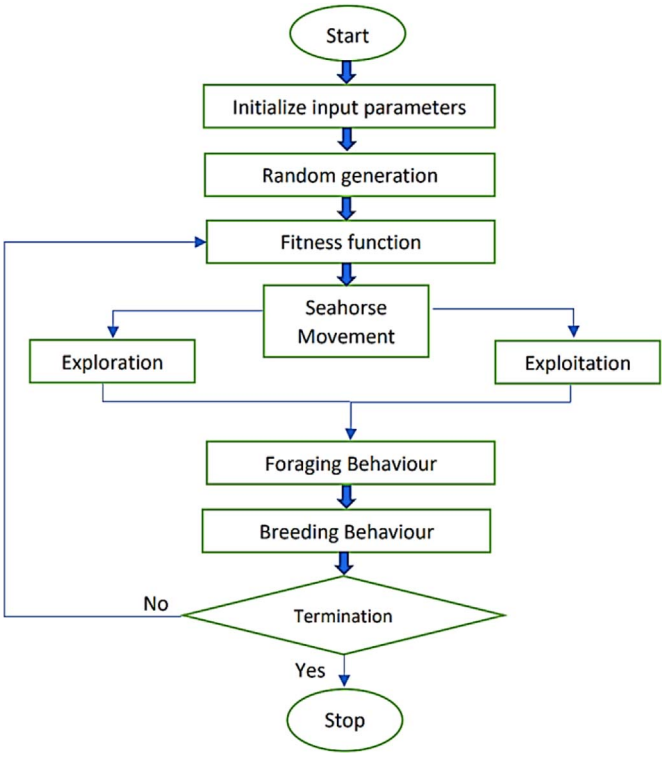


**Fig. 2.** SHO framework.

*Sixth Step:* Breeding Behaviour
Seahorses are split into two gender categories, female and male each group making up 50% of the population during the breeding season.

$$\begin{cases} \text{Father} = Z_{\text{sort}}\left(1 : \frac{\text{pop}}{2}\right) \\ \text{Mother} = Z_{\text{sort}}\left(\frac{\text{pop}}{2} + 1 : \text{pop}\right) \end{cases}. \quad (26)$$

Where:
$Z_{\text{sort}}$= Fitness value.
In the SHO algorithm, each pair produces one child.

$$Z_j = (1 - r_3)Z_{\text{Mother}} + rZ_{\text{Father}}. \quad (27)$$

Where:
$r_3$ = Random number of male and female members by $Z_{\text{Father}}$ and $Z_{\text{Mother}}$.

*Seventh Step:* Termination
Verify the termination conditions; if they are satisfied, it indicates that an optimal solution has been achieved. If not, proceed with repeating the process. Figure 2 depicts the flowchart of SHO.

## 4.2 MDACGAN optimization method

The MDACGAN model employs a CGAN framework, comprising discriminators and generators. The generator network creates varied and lifelike power dispatch solutions, while the discriminator network aims to differentiate between generated and real solutions. GAN provides a unique method in which the correlation between the projected vector P and power dispatch can be harnessed by microgrid $W_{\text{gan}}(M, Q)$ according to equation (28) [44]:

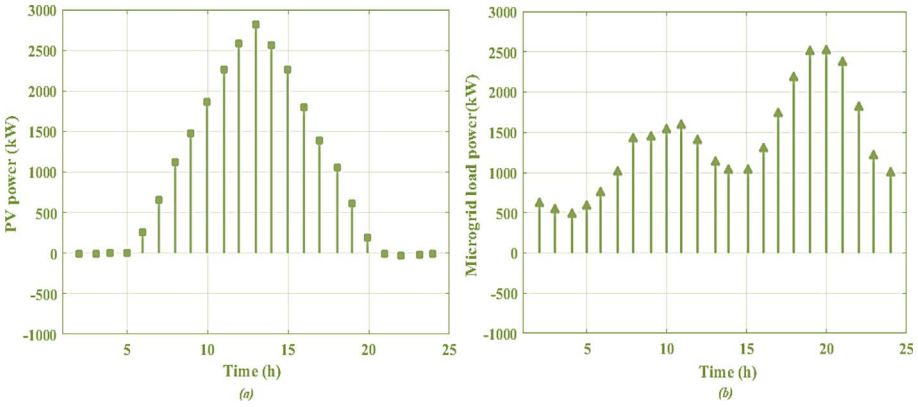


**Fig. 3.** Case 1. (a) PV power and (b) demand of microgrid.

$$W_{\text{gan}}(M, Q) = B_{c\sim \text{Zdata}(c)}[log(Q(c))] + B_{P\sim ZP(P)}[\log(1 - Q(M(P)))]. \quad (28)$$

Where:
$c$ = Power dispatch prediction.
Zdata = Data distribution.
$Q(c)$ = Discriminator output.
$ZP$ = $Z$-distribution.
$M(P)$ = Generator output.

In this research, Conditional GAN is employed to map multiple predicted domains $P$ to a single domain $J$, leading to precise power dispatch prediction denoted in equation (29).

$$W_{x\text{GAN}}(M, Q) = B_{J,I\sim \text{Zdata}(J,I)}[\log Q(J, I)] + B_{J\sim \text{Zdata}(J),P\sim ZP(P)\times}[\log(1 - Q(J, M(J, P)))]. \quad (29)$$

Where:
$P$ = Electricity demand.
$J$ = Predicted data.

The loss function for MACGAN is made up of three separate loss functions, as shown in equation (30).

$$W_{MACGAN} = \arg\min_{M} \max_{Q} W_{x\text{GAN}}(M, Q) + W_{w1}(M) W_{\text{Yff}}. \quad (30)$$

The generator $M$ and the discriminator $Q$ participate in a min-max game where $M$ tries to minimize the above function while $Q$ seeks to maximize it, leading to opposition. The $L$ loss, as depicted, reduces the gap between the actual and predicted power, as shown in equation (31).

$$W_{W1}(M) = \frac{1}{XNL} \sum_{x=1}^{X} \sum_{k=1}^{N} \sum_{j=1}^{L} \gamma_X \left| O_{\text{mf}}^{(j,k,x)} - M(O_{\text{in}})^{(j,k,x)} \right|. \quad (31)$$

The symbols $X$, $L$, and $N$ are used to represent the channel, time, and level of traffic in this case. The third factor is attention loss, which minimizes the difference between the binary function, and is accurately predicted by the optimal allocation of power generation resources for improved prediction as shown in equation (32).

$$W_{\text{Yff}} = \| Y - E \|_2^2. \quad (32)$$

Where:
$Y$ = Map produced by attention module.
$E$ = Unwanted data.

## 5 Case studies and numerical results

Based on the simulation findings, this section demonstrates the performance of the proposed method. The SHO-MDACGAN technique was introduced in this study to minimize power exchange between the microgrid and the main grid, maximize PV power, and reduce costs. The simulation of the proposed SHO-MDACGAN technique is conducted on the MATLAB software, and its performance is compared with various methods. The simulation results are categorized into four cases: Case 1 involves operation with electric vehicle and demand response, Case 2 involves operation with random electric vehicle and demand response, Case 3 involves operation with orderly electric vehicle and non-participation in demand response, and Case 4 involves the analysis of systematic electric vehicle and without participation TL. It should be mentioned, that all data and parameters of this study are extracted from references [45–48].

### Case 1: Operation of microgrid with electric vehicle and demand response

Figure 3 depicts PV power and load demand in case 1. The power starts at 0 kW at 1:00, gradually increasing to a peak of 2800 kW at 13:00, and then decreasing until 24:00. Case 1, Figure 3b illustrates the analysis of microgrid load demand, showcasing time in hours (h) and load demand in kW.

Figure 4 displays the examination of load, along with the uncontrollable demand for electric vehicles and the demand response for electric vehicles. Figure 4a displays uncontrollable demand for electric vehicles, with output power ranging from maximum and minimum 1500 kW. The power diminishes steadily from 5:00 onwards as it discharges until midnight. Figure 4b demonstrates the

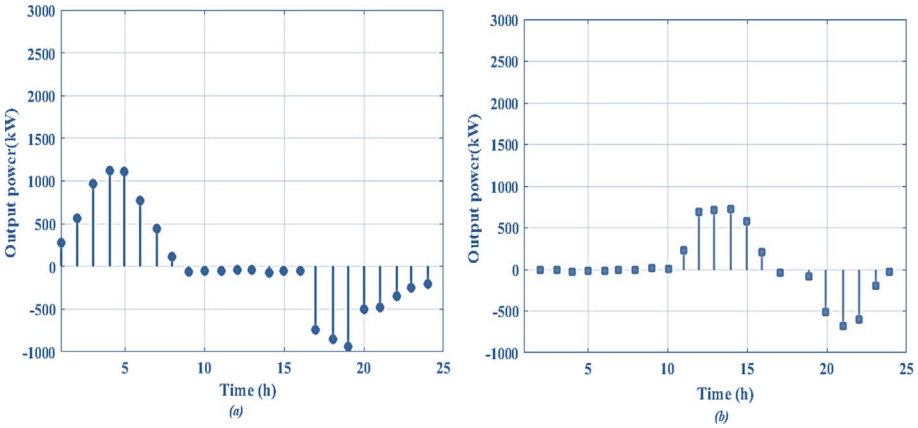


**Fig. 4.** Case 1. (a) Demand of uncontrollable load; (b) Demand of controllable load.

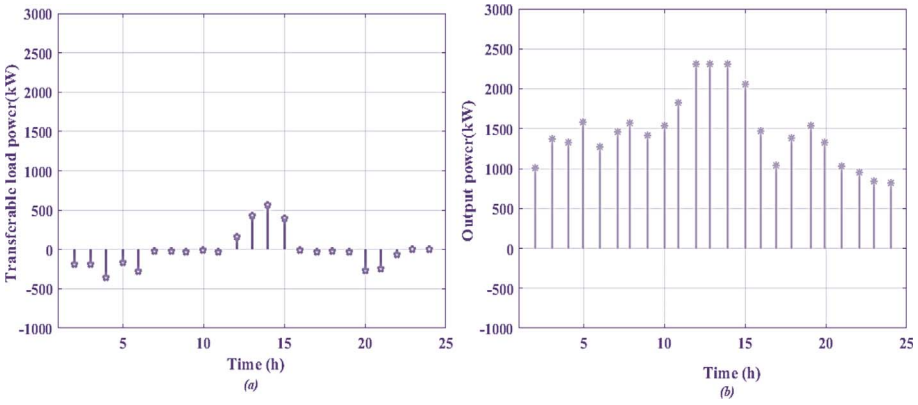


**Fig. 5.** Case 1. (a) Demand of transferable load power; (b) Demand of microgrid with electric vehicle and transferable load.

adjustable demand for electric vehicles, with a power range of −1000 to 1000 kW. The power reaches its peak at 700 kW at 13:00 and then gradually diminishes until 24:00.

Figure 5 illustrates the contrast between load curves for TL power and demand load associated with electric vehicles and TL. The peak value of 600 kW is achieved at 14:00 before gradually decreasing until 24:00. Figure 5b shows the load demand, including electric vehicle and TL. The value diminishes slowly until it reaches 24:00. SOC analysis for an energy storage unit in case 1 is depicted in Figure 6. It commences at 1:00, gradually decreases, and then rises to a peak of 0.9 kW by 17:00.

## Case 2: Operation with random electric vehicle and demand response

Figure 7 depicts PV power and load demand in case 2. The PV power starts at 1:00 and gradually increases to reach 2900 kW at 13:00, then decreases until 24:00. In Figure 7b, the microgrid original load power gradually decreases after 20:00 until 24:00. Figure 8 shows the load demand for electric vehicles and TL in case 2. Figure 8a shows the load demand gradually decreasing after 14:00 until 24:00, while Figure 8b shows the TL power. Figure 8c shows load demand, at 1:00 starting with a value of 1300 kW, gradually increases to reach 3800 kW at 18:00, and then decreases

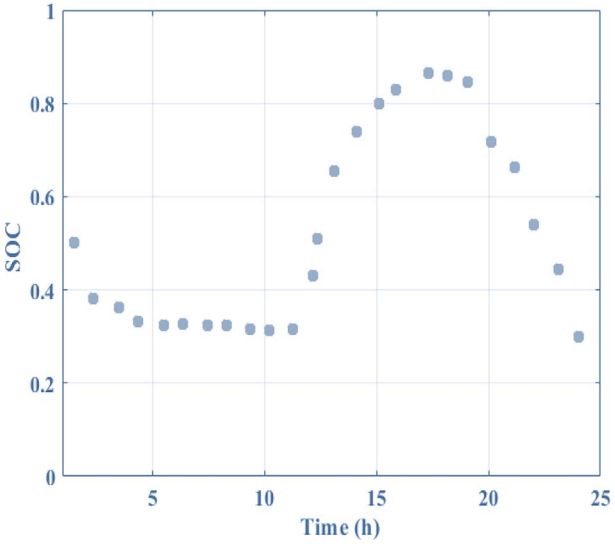


**Fig. 6.** SOC of energy storage system in Case 1.

until 24:00. The SOC for the storage system is shown in Figure 9 starting at 0.5 kW and gradually increasing to a peak of 0.8 kW at 16:00.

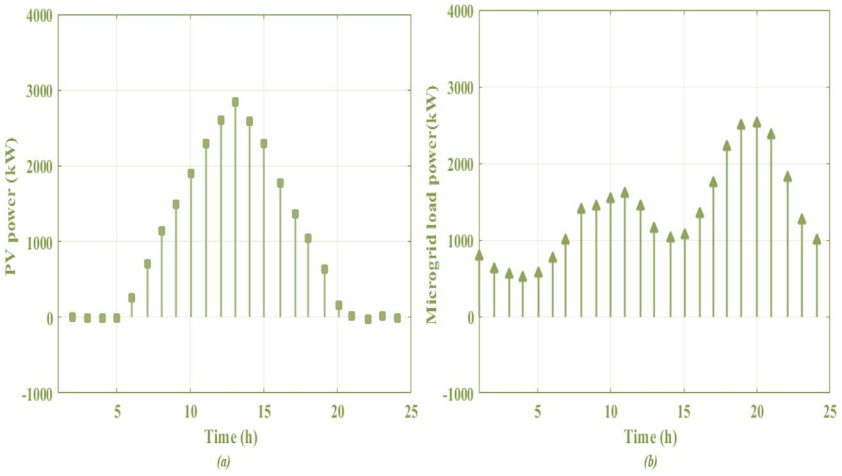


**Fig. 7.** Case 2. (a) PV power and (b) demand of microgrid.

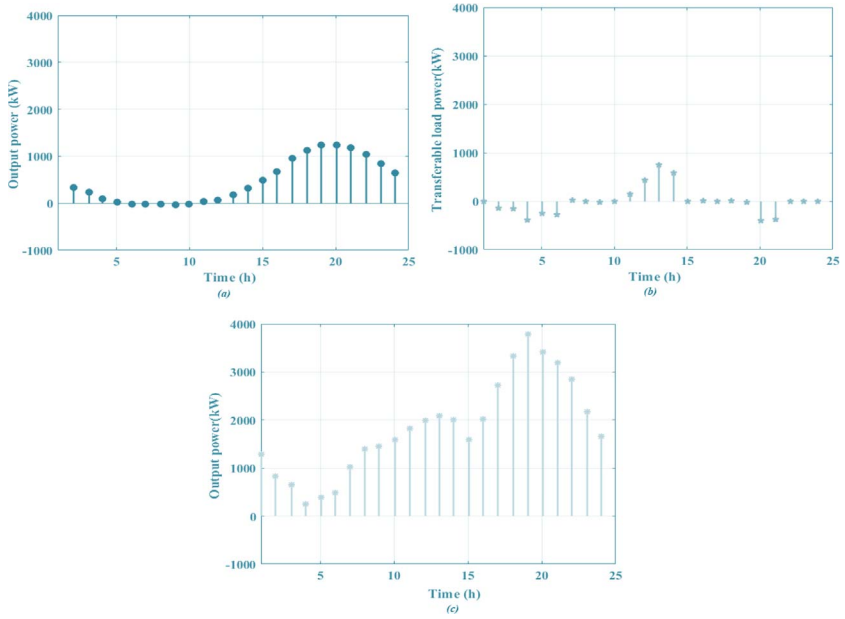


**Fig. 8.** Case 2. (a) Demand of uncontrollable load; (b) Demand of controllable load; (c) Microgrid load.

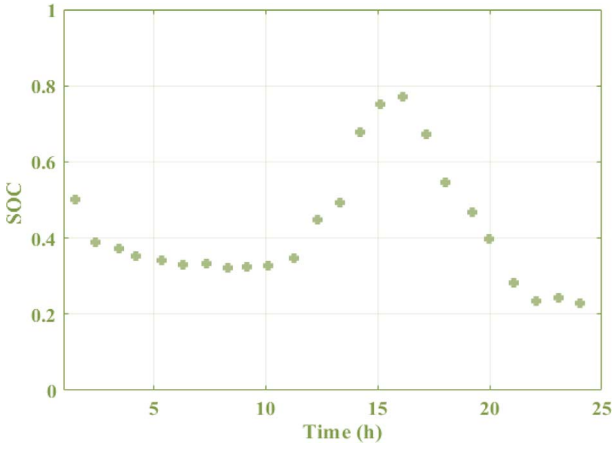


**Fig. 9.** SOC of energy storage system in Case 2.

### Case 3: Operation with orderly electric vehicle and non-participation in demand response

Figure 10 provides PV power and load demand in case 3. Figure 10a showcases the fluctuation of PV power generation throughout the day, starting at 2:00 with a value of 2000 kW and peaking at 13:00 with 2700 kW before gradually decreasing until 24:00. The variation in load demand, starting at 500 kW at 2:00 and then decreasing steadily until the end of the day. In Figure 11, uncontrollable and controllable loads for electric vehicles are depicted, along with the demand. Figure 11a shows the fluctuation of uncontrollable load power for electric vehicles in ranges of 1500 kW. Figure 11b shows the controllable load power for electric vehicles, upper and lower ranges 1000 kW. Figure 11c illustrates the variation in microgrid load power, starting at 1000 kW at 1:00, peaking at 2000 kW at 13:00,

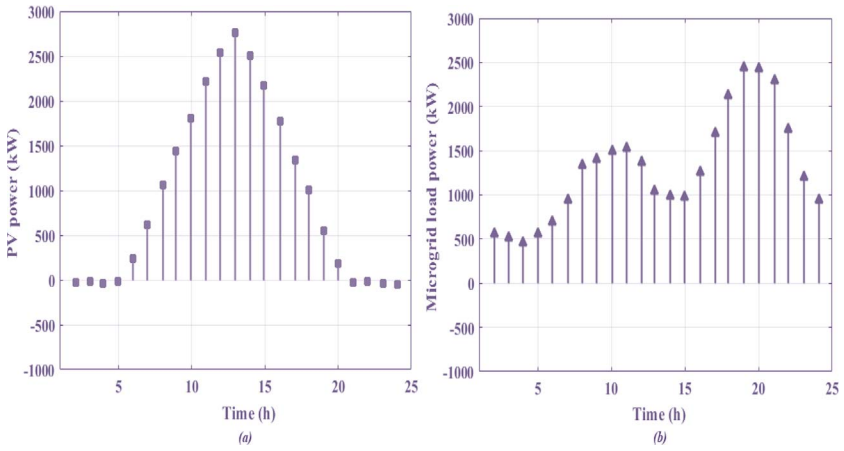


**Fig. 10.** Case 3. (a) PV power and (b) demand of microgrid.

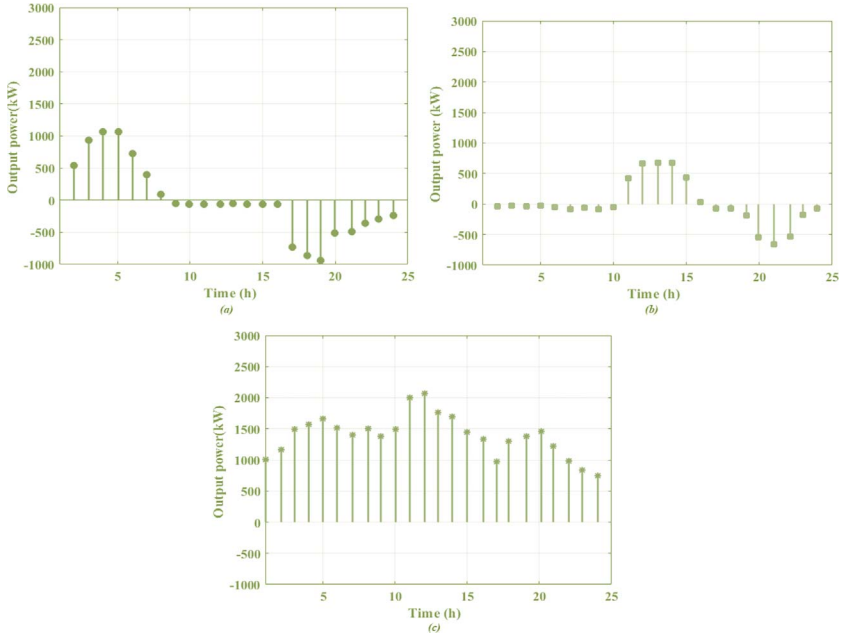


**Fig. 11.** Case 3. (a) Demand of uncontrollable load; (b) Demand of controllable load; (c) Microgrid load.

and gradually decreasing until 24:00. Figure 12 presents the SOC for the storage system. The SOC value initiates at 0.5 kW and rises consistently until it peaks at 1 kW by 18:00, demonstrating the energy storage unit's charging and discharging behaviours over the day.

### Case 4: Operation with systematic electric vehicle and without participation of TL

Figure 13 depicts PV power and load demand in case 4. The initial value is 1200 kW at 1:00, gradually increasing to a peak of 3800 kW at 20:00, then decreasing until 24:00. Figure 13b shows the load demand, starting at 800 kW at 1:00, peaking at 2500 kW at 20:00, and decreasing until 24:00. Figure 14 shows the load demand for electric vehicle charging and load demand of the electric vehicle. Figure 14a displays the analysis of the charging load for electric

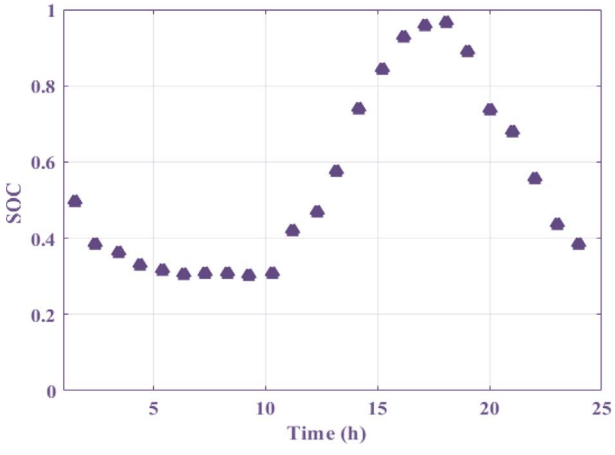


**Fig. 12.** SOC of energy storage system in Case 3.

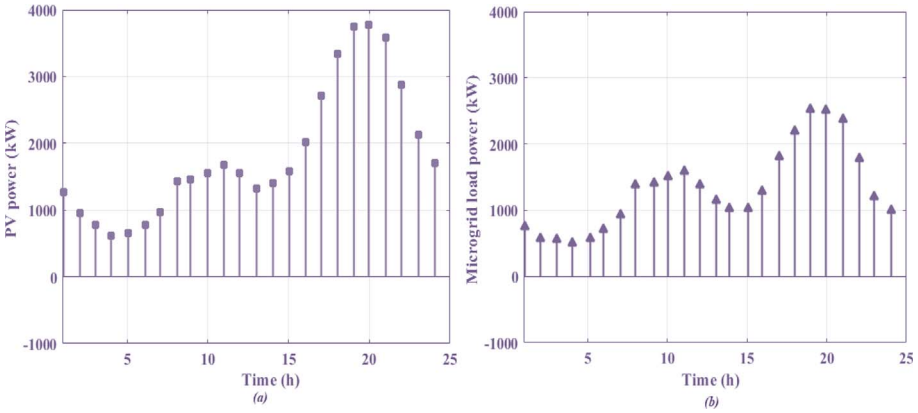


**Fig. 13.** Case 4. (a) PV power and (b) demand of microgrid.

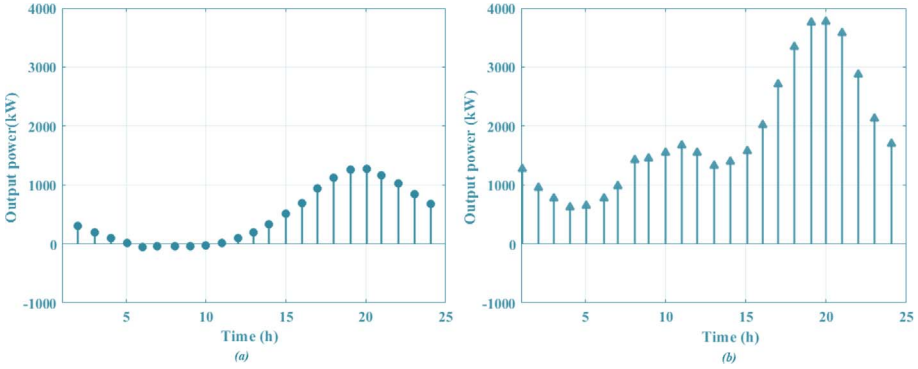


**Fig. 14.** Case 4. (a) Demand of uncontrollable load; (b) Demand of controllable load; (c) Microgrid load.

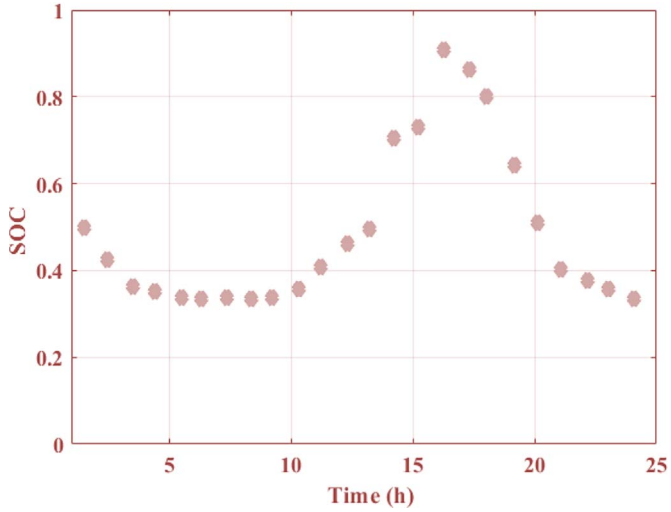


**Fig. 15.** SOC of energy storage system in Case 4.

vehicles, starting at 300 kW at 2:00, peaking at 1200 kW at 20:00, and decreasing until 24:00. Figure 14b shows the load demand for electric vehicle charging, gradually decreasing after 20:00 until 24:00. Figure 15 illustrates SOC curves of storage system starting at 0.5 and peaking at 0.9 kW at 16 h, then gradually decreasing until 24:00.

**Table 1.** Comparison of the proposed algorithm to other algorithms in Case 4.

| Algorithms | Best solution ($) | Worst solution ($) |
|---|---|---|
| HBO | 2.2 | 2.8 |
| PSO | 3.2 | 3.6 |
| SSA | 4.2 | 4.9 |
| Proposed | 1.2 | 1.6 |

In Table 1, a comparison of cost considering the proposed algorithm to other algorithms is listed. The results based on the best and worst values are presented. The obtained results of the proposed algorithm are more optimal than other algorithms.

## 6 Conclusion

This study presented a hybrid approach for the optimal behaviour of electric vehicles and demand management in electrical microgrids. The proposed approaches involve the simultaneous use of the SHO and the MDACGAN techniques. The main objective of this method is to decrease the operational cost and optimize solar energy usage.

The economic system for the microgrid includes electric vehicles, transferable loads, and other energy resources such as energy storage units and PV. The economic dispatch optimization model in the microgrid addresses the variability of renewable energy sources by utilizing the proposed technique to handle uncertainty. The proposed technique shows superior results compared to other methodologies. Furthermore, the SHO-MDACGAN technique allows for the integration of electric vehicles into the microgrid system, enabling efficient management of their charging and discharging patterns. By optimizing the use of solar energy and minimizing power fluctuations, the microgrid can operate more sustainably and cost-effectively. The economic framework considers various factors such as transferable loads and distributed generations, ensuring a comprehensive approach to energy management. Overall, the research highlights the potential benefits of the SHO-MDACGAN technique in enhancing the performance of PV microgrid systems. By effectively managing the variability of renewable energy sources and optimizing the use of electric vehicles, this approach offers a promising solution for reducing operational expenses and improving overall efficiency. The findings of this study contribute to the growing body of research on sustainable energy management and provide valuable insights for future developments in the field. Based on the results, it can be concluded that the suggested technique offers a lower cost compared to other methods.

## References


1 Narasipuram R.P., Mopidevi S. (2024) Assessment of E-mode GaN technology, practical power loss, and efficiency modelling of iL2C resonant DC-DC converter for xEV charging applications, *J. Energy Storage* **91**, 112008.

2 Narasipuram R.P., Mopidevi S. (2021) A technological overview & design considerations for developing electric vehicle charging stations, *J. Energy Storage* **43**, 103225.

3 Banothu C.S., Gorantla S.R., Attuluri R.V.B., Evuri G.R. (2024) Impacts of wireless charging system for electric vehicles on power grid, *e-Prime Adv. Electr. Eng. Electr. Energy* **8**, 100561.

4 Ghorbani M., Wang H., Roberts N. (2024) Analytical and numerical modeling of phase change material and hybrid PCM-heat sinks for high-power wireless EV charging, *Int. Commun. Heat Mass Transf.* **154**, 107460. https://doi.org/10.1016/j.icheatmasstransfer.2024.107460.

5 Souri J., OmidvarMohammadi H., Neyshabouri S.A.A.S., Chooplou C.A., Kahrizi E., Akbari H. (2024) Numerical simulation of aeration impact on the performance of a-type rectangular and trapezoidal piano key weirs, *Model. Earth Syst. Environ.* **10**, 5205–5224. https://doi.org/10.1007/s40808-024-02058-4.

6 Zarean Dowlat Abadi J., Iraj M., Bagheri E., Rabiei Pakdeh Z., Dehghani Tafti M.R. (2022) A multiobjective multiproduct mathematical modeling for green supply chain considering location-routing decisions, *Math. Probl. Eng.* **2022**, 1, 7009338. https://doi.org/10.1155/2022/7009338.

7 Panahi S., Cheraghifar F., Talebian Sh. (2018) An investigation on painting and imagery in zen, *Mod. Appl. Sci* **12**, 9, 200–208.

8 Ghorbani M., Wang H. (2023) Computational modeling and experiment validation of a microchannel cross-flow heat exchanger, *Int. Commun. Heat Mass Transf.* **149**, 107116. https://doi.org/10.1016/j.icheatmasstransfer.2023.107116.

9 Kahrizi E., Neyshabouri S.A.A.S., Zeynolabedin A., Souri J., Akbari H. (2023) Experimental evaluation of two-layer air bubble curtains to prevent seawater intrusion into rivers, *J. Water Clim. Change* **14**, 2, 543–558. https://doi.org/10.2166/wcc.2023.384.

10 Iraj M., Chobar A.P., Peivandizadeh A., Abolghasemian M. (2024) Presenting a two-echelon multi-objective supply chain model considering the expiration date of products and solving it by applying MODM, *Sustain. Manuf. Serv. Econ.* **3**, 100022. https://doi.org/10.1016/j.smse.2024.100022.

11 Javidialsaadi A., Mondal S., Subramanian S. (2023) Model checks for two-sample location-scale, *J. Nonparametr. Stat.* **36**, 3, 749–779. https://doi.org/10.1080/10485252.2023.2243350.

12 Chen D., Hosseini A., Smith A., Nikkhah A.F., Heydarian A., Shoghli O., Campbell B. (2024) *Performance evaluation of real-time object detection for electric scooters*. arXiv preprint https://doi.org/10.48550/arXiv.2405.03039.

13 Atashpanjeh H., Behfar A., Haverkamp C., Verdoes M.M., Al-Ameen M.N. (2022) Intermediate help with using digital devices and online accounts: understanding the needs, expectations, and vulnerabilities of young adults, in: A. Moallem (ed), *HCI for Cybersecurity, Privacy and Trust. HCII 2022. Lecture Notes in Computer Science*, vol. **13333**, Springer, Cham, pp. 3–15. https://doi.org/10.1007/978-3-031-05563-8_1.

14 EskandariNasab M., Raeisi Z., Lashaki R.A., Najafi H. (2024) A GRU-CNN model for auditory attention detection using microstate and recurrence quantification analysis, *Sci. Rep.* **14**, 8861. https://doi.org/10.1038/s41598-024-58886-y.

15 Nguyen V.D., Mirza S., Zakeri A., Gupta A., Khaldi K., Aloui R., Mantini P., Shah S.K., Merchant F., Merchant F. (2024) Tackling domain shifts in person re-identification: a survey and analysis, in: *Proceedings of the IEEE/CVF Conference on Computer Vision and Pattern Recognition*, pp. 4149–4159.

16 Kiani S., Salmanpour A., Hamzeh M., Kebriaei H. (2024) Learning robust model predictive control for voltage control of islanded microgrid, *IEEE Trans. Autom. Sci. Eng.* https://doi.org/10.1109/TASE.2024.3388018.

17 Seifi N., Al-Mamun A. (2024) Optimizing memory access efficiency in CUDA kernel via data layout technique, *J. Comput. Commun.* **12**, 124–139. https://doi.org/10.4236/jcc.2024.125009.

18 Behfar A., Atashpanjeh H., Al-Ameen M.N. (2023) Can password meter be more effective towards user attention, engagement, and attachment? A study of metaphor-based designs, in: *Companion Publication of the 2023 Conference on Computer Supported Cooperative Work and Social Computing*, pp. 164–171. https://doi.org/10.1145/3584931.3606983.

19 Zakeri A., Hassanpour H. (2021) Whispernet: deep siamese network for emotion and speech tempo invariant visual-only lip-based biometric, in: *2021 7th International Conference on Signal Processing and Intelligent Systems (ICSPIS)*, IEEE, pp. 1–5. https://doi.org/10.1109/ICSPIS54653.2021.9729394.

20 Hosseini A., Yahouni Z., Feizabadi M. (2023) Scheduling AIV transporter using simulation-based supervised learning: a case study on a dynamic job-shop with three workstations, *IFAC – Pap.* **56**, 2, 8591–8597. https://doi.org/10.1016/j.ifacol.2023.10.032.

21 Hajrasouliha A., Ghahfarokhi B.S. (2021) Dynamic geo-based resource selection in LTE-V2V communications using vehicle trajectory prediction, *Comput. Commun.* **177**, 239–254.

22 Akbari P., Bafarasat A.Z. (2024) Exploring energy efficiency in historical urban fabrics for energy-conscious planning of new urban developments, *J. Urban Plan. Dev.* **150**, 2, 04024011.

23 Demir N., Shadjou A.M., Abdulameer M.K., Almasoudie N. K.A., Mohammed N., Fooladi H. (2024) A low-carbon multigeneration system based on a solar collector unit, a bio waste gasification process and a water harvesting unit, *Int. J. Low-Carbon Technol.* **19**, 1204–1214.

24 Ashary A., Rayguru M.M., SharafianArdakani P., Kondaurova I., Popa D.O. (2024) Multi-joint adaptive motion imitation in robot-assisted physiotherapy with dynamic time warping and recurrent neural networks, in: SoutheastCon 2024, Atlanta, GA, USA, 15-24 March, IEEE, pp. 1388 –1394.

25 Yousefizad M., Zarasvand M.M., Bagheritabar M., Ghezelayagh M.M., Farahi A., Ghafouri T., Raissi F., Zeidabadi M. A., Manavizadeh N. (2023) Performance investigation of low-power flexible n-ZnO/p-CuO/n-ZnO heterojunction bipolar transistor: simulation study, *Micro Nanostructures* **180**, 207594.

26 Ghasemi E., Ranjbaran A., Pourhossein J. (2023) Designing multi-objective electric and thermal energy management system of microgrid in the presence of controllable loads and electric vehicles, *Electr. Eng.* **106**, 2, 1–14.

27 Gholami K., Abbasi M., Azizivahed A., Li L. (2023) An efficient bi-objective approach for dynamic economic emission dispatch of renewable-integrated microgrids, *J. Ambient Intell. Humaniz. Comput.* **14**, 8, 10695–10714.

28 Tong L., Zhao S., Jiang H., Zhou J., Xu B. (2021) Multi-scenario and multi-objective collaborative optimization of distribution network considering electric vehicles and mobile energy storage systems, *IEEE Access* **9**, 55690–55697.

29 Heydari A., Nezhad M.M., Keynia F., Fekih A., Shahsavari-Pour N., Garcia D.A., Piras G. (2023) A combined multi-objective intelligent optimization approach considering techno-economic and reliability factors for hybrid-renewable microgrid systems, *J. Clean. Prod.* **383**, 135249.

30 Hou H., Wang Q., Xiao Z., Xue M., Wu Y., Deng X., Xie C. (2022) Data-driven economic dispatch for islanded microgrid considering uncertainty and demand response, *Int. J. Electr. Power Energy Syst.* **136**, 107623.

31 Cao Y., Mu Y., Jia H., Yu X., Hou K., Wang H. (2024) A multi-objective stochastic optimization approach for planning a multi-energy microgrid considering unscheduled islanded operation, *IEEE Trans. Sustain. Energy* **15**, 1300–1314.

32 Wang R., Xu T., Xu H., Gao G., Zhang Y., Zhu K. (2023) Robust multi-objective load dispatch in microgrid involving unstable renewable generation, *Int. J. Electr. Power Energy Syst.* **148**, 108991.

33 Mukhopadhyay B., Das D. (2022) Optimal multi-objective long-term sizing of distributed energy resources and hourly power scheduling in a grid-tied microgrid, *Sustain. Energy Grids Netw.* **30**, 100632.

34 Qiao B., Liu J., Huan J. (2022) Multi-objective economic emission dispatch of thermal power-electric vehicles considering user's revenue, *Soft Comput.* **26**, 22, 12833–12849.

35 Chen H., Gao L., Zhang Z. (2021) Multi-objective optimal scheduling of a microgrid with uncertainties of renewable power generation considering user satisfaction, *Int. J. Electr. Power Energy Syst.* **131**, 107142.

36 Tian H., Wang K., Cui X., Chen Z., Zhao E., Saeedi S. (2023) Multi-objective planning of microgrid based on renewable energy sources and energy storage system, *J. Energy Storage* **68**, 107803.

37 Tan B., Chen H., Zheng X., Huang J. (2022) Two-stage robust optimization dispatch for multiple microgrids with electric vehicle loads based on a novel data-driven uncertainty set, *Int. J. Electr. Power Energy Syst.* **134**, 107359.

38 Asaad A., Ali A., Mahmoud K., Shaaban M.F., Lehtonen M., Kassem A.M., Ebeed M. (2023) Multi-objective optimal planning of EV charging stations and renewable energy resources for smart microgrids, *Energy Sci. Eng.* **11**, 3, 1202–1218.

39 Chamandoust H., Hashemi A., Bahramara S. (2021) Energy management of a smart autonomous electrical grid with a hydrogen storage system, *Int. J. Hydrogen Energy* **46**, 17608–17626. https://doi.org/10.1016/j.ijhydene.2021.02.174.

40 Xu Y.P., Liu R.H., Tang L.Y., Wu H., She C. (2022) Risk-averse multi-objective optimization of multi-energy microgrids integrated with power-to-hydrogen technology, electric vehicles and data center under a hybrid robust-stochastic technique, *Sustain. Cities Soc.* **79**, 103699.

41 Chamandoust H. (2022) Optimal hybrid participation of customers in a smart micro-grid based on day-ahead electrical market, *Artif. Intell. Rev.* **55**, 5891–591. https://doi.org/10.1007/s10462-022-10154-z.

42 Chamandoust H., Derakhshan G., Hakimi S.M., Bahramara S. (2019) Tri-objective scheduling of residential smart electrical distribution grids with optimal joint of responsive loads with renewable energy sources, *J Energy Storage* **27**, 101112. https://doi.org/10.1016/j.est.2019.101112.

43 Özbay F.A. (2023) A modified seahorse optimization algorithm based on chaotic maps for solving global optimization and engineering problems, *Eng. Sci. Technol. Int. J.* **41**, 101408.

44 Sharma P., Kumar M., Sharma H.K., Biju S.M. (2024) Generative adversarial networks (GANs): introduction, taxonomy, variants, limitations, and applications, *Multimed. Tools Appl.* 1–48.

45 Chamandoust H., Bahramara S., Derakhshan G. (2020) Multi-objective operation of smart stand-alone microgrid with the optimal performance of customers to improve economic and technical indices, *J. Energy Storage* **31**, 101738. https://doi.org/10.1016/j.est.2020.101738.

46 Chamandoust H., Derakhshan G., Hakimi S.M., Bahramara S. (2019) Tri-objective optimal scheduling of smart energy hub system with schedulable loads, *J. Clean. Prod.* **236**, 117584. https://doi.org/10.1016/j.jclepro.2019.07.059.

47 Sun S., Wang C., Wang Y., Zhu X., Lu H. (2022) Multi-objective optimization dispatching of a micro-grid considering uncertainty in wind power forecasting, *Energy Rep.* **8**, 2859–2874.

48 Nazir M.S., Almasoudi F.M., Abdalla A.N., Zhu C., Alatawi K.S.S. (2023) Multi-objective optimal dispatching of combined cooling, heating and power using hybrid gravitational search algorithm and random forest regression: towards the microgrid orientation, *Energy Rep.* **9**, 1926–1936.